A Mechanistic Model of Ca Regulation of Thin Filaments in Cardiac Muscle

Nadia A. Metalnikova and Andrey K. Tsaturyan*

Supporting materials

Shape of the Tm chain pinned in a single point

General solution of Eq. A2 is given in Eq. A3 for an infinitely long chain pinned in one site to $\varphi = 1$ is given in Appendix (Eq. A4). Plots of this solution for different values of $\beta \geq 0$ are shown in Fig. S1.

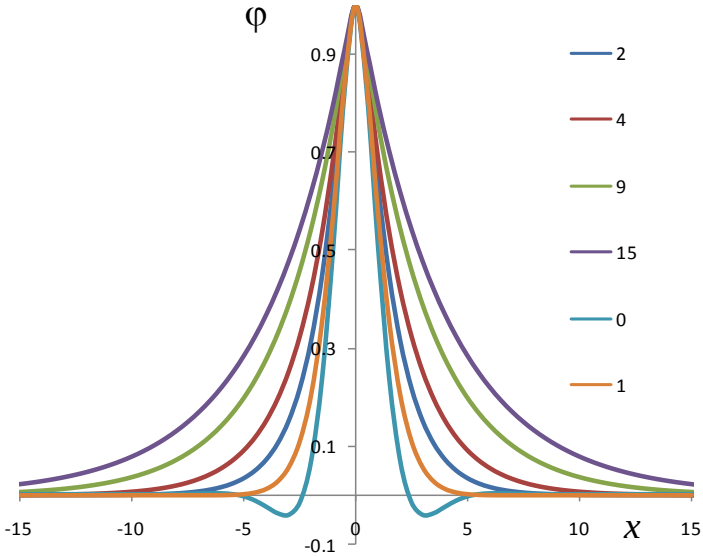

Fig. S1. Configurations of infinitely long Tm chain pinned at x = 0 to φ = 1 for different β values (shown next to the plot for lines of different colors).

Two- and three-pin approximations

The two- and three-pin problems were also solved using general solution (Eq. A3) with the following boundary conditions in each of the pin points, x_0, where the pin angle is φ_*: $\varphi(x_0 - 0) = \varphi(x_0 + 0) = \varphi_*$, $\varphi'(x_0 - 0) = \varphi'(x_0 + 0)$, $\varphi"(x_0 - 0) = \varphi"(x_0 + 0)$. The boundary conditions in infinity are: $\varphi(x) \to 0, \varphi'(x) \to 0$, when $x \to \infty$ or $x \to -\infty$. The problems were reduced to a system of four linear equations with four unknowns in the case of two-pin chain and to a system of twelve equations with twelve unknowns in the case of three pin points. These problems were solved by a computer for every possible combination of pin elements: troponins and myosins and all possible distances between them. Calculated energies were then used during Monte-Carlo simulations.

We used three-point approximation instead of two-point approximation because in some cases the difference between them was significant and three pin point approximation was more accurate and precise (Fig. S2). Two-pin approximation was obtained assuming that Tm chain configuration between every two neighbor pin points is

the same as for an infinitely long chain pinned in these two points only (refs. 7-10). For three-point approximation we calculated changes in configuration and energy of a Tm chain pinned in two points (nearest neighbors) upon pinning in an intermediate point. The difference between these two approaches is illustrated by Fig. S2.

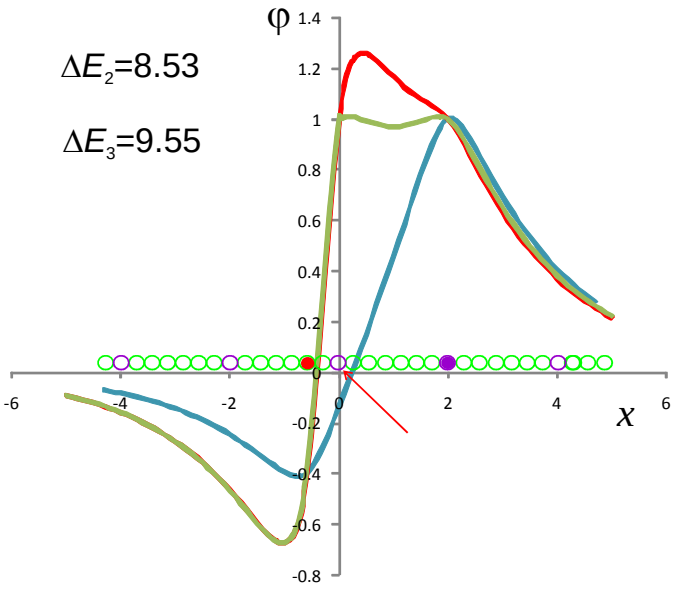

Fig. S2. An example showing the difference between the two- and three-point approximations. Actin monomers are shown schematically by green circles, purple empty circles correspond to actin sites covered by Tn, TnI bound to actin are shown as solid purple circles, actin site occupied by bound myosin heads are red. An infinitely long chain pinned by a myosin head and a TnI molecule is shown in blue. Green and red lines show the Tm configuration obtained for two- and three-point approximations, respectively, when the chain additionally pinned at $x = 0$. The difference in dimensionless energies upon TnI pinning at origin for two-pin approximation is ΔE_2. The same value obtained for three-pin approximation is ΔE_3. The difference between them is as high as 1.02.

We also tested how the addition of an extra pin point outside close neighborhood affects energy changes upon Tm pinning to actin (Fig. S3). For this we used four-point approximation and checked whether the three-point approximation is good enough. The difference between the three- and four point approximations was in most cases small and could be neglected. For example the addition of a TnI or myosin pin outside the nearest neighborhood caused a difference in calculated energy changes of <0.08 only (Fig. S3). These examples show that our three-pin approximation is good enough for effective estimation of changes in energy of Tm chain caused by binding or unbinding of TnI or myosin to actin.

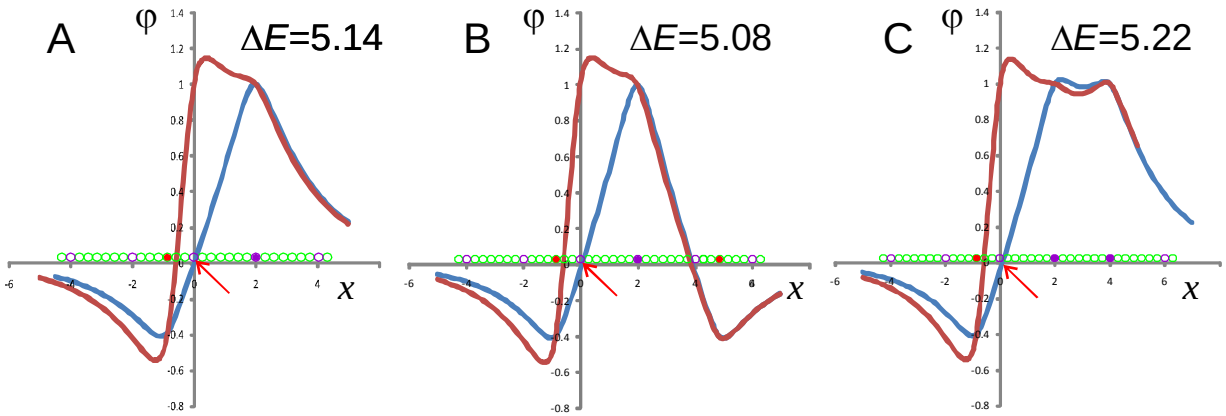

Fig. S3. An example showing the difference between the three- and four-point approximations. Actin monomers are shown schematically by green circles, purple empty circles correspond to actin sites covered by Tn. TnI bound to actin are shown as solid purple circles, actin site occupied by bound myosin heads are red. Blue and red lines show Tm chain configuration before its pinning at $x = 0$ (red arrow) and after it, respectively. In B and C additional myosin or TnI pin point was added on the right.

Effect of parameter ε on Ca-activation

In the calculation presented in Figs. 4-7 we set parameter ε to zero. This means that the mobile segment cannot bind hydrophobic pocket of TnC unless TnC binds Ca^{2+}. The effect of parameter ε on Ca-curves for normalized concentration of the TnI-actin and CaTnC complexes in our model is shown in Fig. 4S.

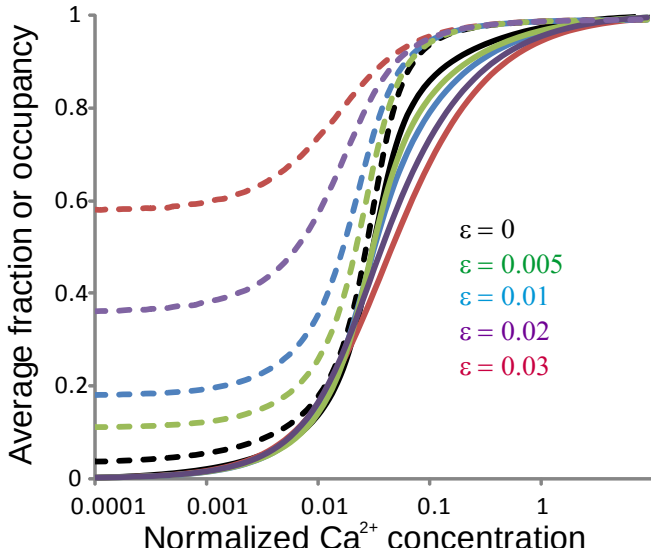

Fig. S4. The calculated model Ca curves in the absence of myosin heads for different values of ε (shown in the plot). The average calculated fractions of actin-unbound TnI are shown by dashed lines and the occupancies of TnC sites by Ca^{2+} ions are shown by continuous lines.

As one would expect calculations show that an increase in ε leads to an increase in the fraction of TnI which are not bound to actin even in the absence of calcium so that the dynamic range of Ca regulation of the thin filaments decreases. Besides, an increase in ε causes a decrease in the cooperativity of the Ca curves.

Effect of parameter γ on Ca-activation

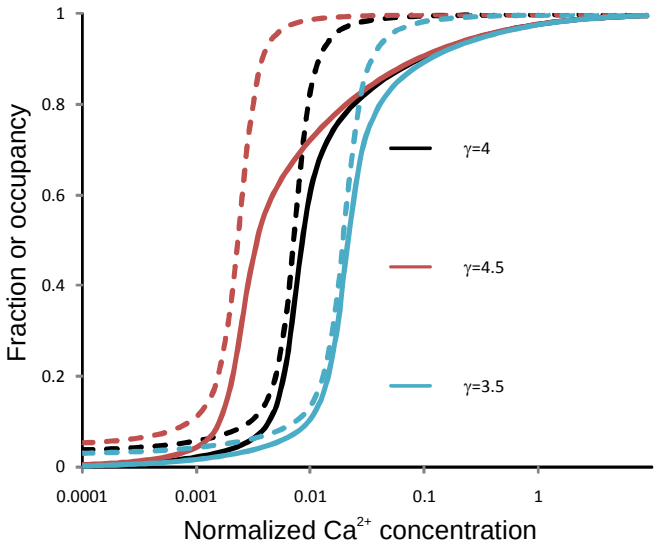

Fig. S5. The calculated model Ca curves in the absence of myosin heads for different values of γ (shown in the plot). The average calculated fractions of actin-unbound TnI are shown by dashed lines and the occupancies of TnC sites by Ca^{2+} ions are shown by continuous lines.

Effect of 14.5 nm axial repeat of myosin heads on actin on Ca-activation

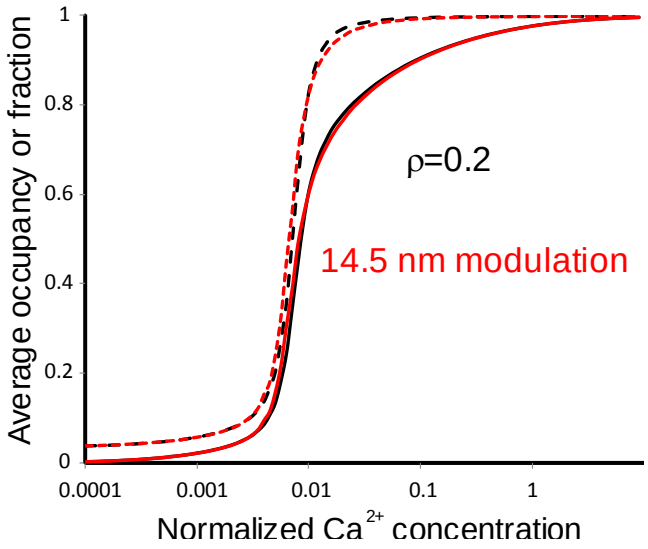

Fig. 6S. The calculated model Ca curves at a constant availability of myosin heads (ρ = 0.2, black) and in the case of its 14.5 nm axial modulation (red). The availability was a sum of 50 Gaussian distributions with their peaks separated by 14.5 nm. The average availability was also 0.2, the full range was 0.08-0.33. The average calculated fractions of actin-unbound TnI are shown by dashed lines and the occupancies of TnC sites by Ca^{2+} ions are shown by continuous lines.

Table S1. **Meanings and values of the model parameters.**

Parameter	***Description***	***Values***
a	Radius at which Tm chain sits on F-actin	4 nm
ψ	Helical twist of unpinned Tm chain ($2\pi/72$ nm)	0.0873 nm^{-1}
K^*	Bending stiffness of the tropomyosin chain	≈ 3600 pN ×nm^2
α	Strength of the chain confining potential	≈ 1.5 pN
ξ	Persistent lengths of Tm-Tn confined chain	19.25 nm (16-24 nm)
β	Dimensionless helicity parameter	0, 2.7-4.2
χ	The ratio of myosin and TnI pinning angles	0.4 (=10°/25°)
E_T	The total energy of a Tm chain pinned by a TnI molecule	
kB, T	The Boltzmann constant, absolute temperature	k_BT≈ 4 pN×nm
γ	Dimensionless energy parameter (=E_T/k_BT)	4 (3.5-4.5)
c	Axial repeat of Tn complexes	38.5 nm
λ	Dimensionless energy parameter, $\lambda = c/\xi$	1.6, 2, 2.4
K_{Ca}	Equilibrium constant for Ca^{2+} binding to TnC.	
K_I	Equilibrium constant for TnI binding to TnC	1000
K_A	Equilibrium constant for TnI binding to actin	200
C	$C = K_{Ca}[Ca^{2+}]$ – dimentionless Ca^{2+} concentration	$[10^{-6};10]$
ε	Constant	0 (up to 0.03)
ρ	Effective affinity of myosin heads for actin	0-0.2
k_{M+}, k_{M-}	Forwards and backward rate constants for myosin binding to actin	
k_{TnI+}, k_{TnI-}	Forward and backward rate constants for TnI binding to actin	

* Bending stiffness value *K* for the Tm chain sliding on the actin surface was estimated to be twice higher that that obtained from MD simulation in solution due to reduced degree of freedom.